

Preparation and mechanical properties of bacterial cellulose nanocomposites loaded with silica nanoparticles

Shoichiro Yano · Hideaki Maeda · Megumi Nakajima ·
Toshiki Hagiwara · Takashi Sawaguchi

Received: 16 May 2007 / Accepted: 23 July 2007 / Published online: 17 August 2007
© Springer Science+Business Media B.V. 2007

Abstract Bacterial cellulose (BC), which is produced by *Gluconacetobacter xylinus* (*Ga. xylinus*) in culture, is made up of a three-dimensional network of ribbon-shaped bundles of cellulose microfibrils. In the current studies, we used two processes to prepare nanocomposites of BC filled with silica particles. In Process I, *Ga. xylinus* was incubated in medium containing silica sol Snowtex 0 (ST 0, pH 2–4) or Snowtex 20 (ST 20, pH 9.5–10.0). The elastic modulus at 20 °C was improved by keeping the amount of silica in the nanocomposites below 4% when ST 20 was used and below 8.7% when ST 0 was used. This process allowed incorporation of 50% silica in BC. Inclusion of higher amounts of silica reduced the modulus at 20 °C and the strength of the nanocomposites below that of BC. X-ray diffraction measurements revealed that the silica particles disturb the formation of ribbon-shaped fibrils and affect the preferential orientation of the (1 $\bar{1}$ 0) plane. We also produced BC-silica nanocomposites by Process II, wherein the BC hydrogel was immersed in different concentrations of silica sols, allowing silica particles to diffuse into the BC hydrogel and lodge in the spaces between the ribbon-shaped fibrils. This

method increased the modulus at 20°C and the strength compared to the BC matrix, but it was difficult to load the BC with more than 10% silica in this way.

Keywords Bacterial cellulose · Silica sol · Nanocomposite · Dynamic viscoelasticity · Tensile strength · X-ray diffractometry

Introduction

Bacterial cellulose (BC) is a unique material produced by the rod-shaped Gram-negative bacterium *Gluconacetobacter xylinus* (*Ga. xylinus*). During cultivation, the bacteria synthesize fine sub-elementary cellulose fibrils, which are extruded from terminal enzyme complexes into the culture medium. Nascent cellulose extending from terminal enzyme complexes is initially amorphous and is gradually crystallized to cellulose I (Haigler et al. 1980; Kai 1989; Takai 1988). The sub-elementary fibrils are approximately 2–4 nm in diameter and are assembled into microfibrils. These microfibrils are then bundled to form ribbon-shaped fibrils of approximately 4 × 80 nm (Iguchi et al. 2000; Tokoh et al. 1998). When the microfibrils are bundled into ribbons, they are aligned parallel to the membrane surface causing the (1 $\bar{1}$ 0) plane to also preferentially orient parallel to the membrane surface (Takai 1988 and 1994; Tokoh et al. 1998). These microstructures affect the

S. Yano (✉) · H. Maeda · M. Nakajima ·
T. Hagiwara · T. Sawaguchi
College of Science and Technology, Nihon University,
1-8-14 Kanda-surugadai, Chiyoda-ku, Tokyo 101-8308,
Japan
e-mail: yano@chem.cst.nihon-u.ac.jp

mechanical properties of BC (Romano et al. 1992). For example, the modulus of elasticity is higher than 10 GPa over a wide temperature range (20–250 °C). The tensile strength of BC is 100–260 MPa, which is comparable to engineering polymers (Iguchi et al. 2000; Yamanaka et al. 1989, 1998).

Because BC is also nontoxic and biodegradable, its use has been examined in a variety of applications. For example, it has been used as a material for diaphragms in speakers and headphones (Iguchi et al. 2000; Yamanaka et al. 1989 and Ichikawa 1995) and as artificial skin for burn or wound healing (Fontana et al. 1990). Also, in Indonesia and the Philippines, BC is manufactured in large quantity as a food called *Nata de coco*. Additional potential uses of BC include use in separation membranes (Takai 1994), paper making (Shibazaki et al. 1994; Yamanaka et al. 1989; Watanabe and Yamanaka 1992; Hioki et al. 1995), and production of electroconductive carbon film (Yoshino et al. 1991).

Recently, various attempts have been made to produce BC composites to develop high functional materials. For instance, water-soluble polymers can be incorporated into BC by adding them to the culture medium for *Ga. xylinus*. BC composites with hemi-celluloses such as xyloglucan, glucomannan, acetylglucomannan, glucuronoxylan, xylan, and pectin have been widely studied as models of plant cell walls (Azuma 1999; Iwata et al. 1998; Hayashi et al. 1987; Atalla et al. 1993; Tokoh et al. 1998, 2002; Astley et al. 2003). Also, water soluble polymers such as polyethylene glycol (PEG), carboxymethyl cellulose (CMC), methyl cellulose (MC), hydroxypropyl cellulose (HPC), and poly(vinyl alcohol) can be incorporated into BC by adding them to the culture medium (Kai and Kobayashi 1992; Takai 1994; Tajima et al. 1995; Seifert et al. 2004). Compared with HEC or MC, it is difficult to introduce HPC having larger substituent groups into BC (Tajima 1999). The modulus of elasticity of BC composites is 1–3 times higher than that of BC itself (Tajima et al. 1995). Glass fiber reinforced BC has been produced by mixing glass fiber together with BC fragments. In this case, SEM shows that BC fragments were trapped on and bound to the surface of the glass fibers (Iguchi et al. 2000). In our previous paper, BC/silica nanocomposites have been produced by a sol–gel process employing tetraethoxysilane, which mimics the biomineralization process in plants (Maeda et al. 2006).

In the current study, we produced cellulose/silica nanocomposites by incorporating silica nanoparticles into BC by two different processes. In the first process (Process I), silica nanoparticles were incorporated in BC hydrogels by adding silica sol to the medium for *Ga. xylinus*. In the second process (Process II), a previously produced BC hydrogel was soaked with silica sol, allowing the silica particles to penetrate the BC. The BC hydrogel/silica composites obtained by these two processes were hot-pressed to obtain dry BC/silica nanocomposite sheets, and their mechanical properties were compared.

Methods

Preparation of BC

Culture medium was prepared by dissolving 15 g of glucose, 2.5 g of polypeptone, 0.5 g of $\text{MgSO}_4 \cdot 7\text{H}_2\text{O}$, 2.5 g of yeast extract, and an approximate amount of vitamins (NEO M.V.I-9; SSP Co. Ltd.) in 500 ml of water. The medium was sterilized by heating it at 120 °C for 9 min in an autoclave, after which it was mixed with 0.5% ethanol and 0.5 g of mannitol. *Ga. xylinus* (IFO 13772) cells were grown under static conditions in a cylindrical glass vessel (100 mm diameter \times 60 mm) at 30 °C for 25 days. First, the solution became turbid, a pellicle appeared on the surface of the liquid and pellicle thickness increased gradually, reaching 20–30 mm after 25 days. The obtained BC hydrogel was washed in water, immersed in 1% aqueous NaOH for 1 day, followed by 1% aqueous $\text{NaClO} \cdot 5\text{H}_2\text{O}$ for 1 day.

Preparation of BC/silica nanocomposite

Silica sol, which is a suspension of approximately 20 wt% silica nanoparticles in water, was used for preparation of BC/silica nanocomposites. The silica sols included Snowtex 0 (ST 0) and Snowtex 20 (ST 20) (Nissan Chemical Industries, Ltd.). The silica particles have a diameter of 10–20 nm, and the pH of ST 20 and ST 0 were 9.5–10.0 and 2–4, respectively. BC nanocomposites were prepared by two processes, which we referred to as Processes I and II. In Process I, 0.05–2 wt% silica sol was added to the culture medium, and the cells were cultured at 30 °C for

25 days. In this case, $\text{MgSO}_4 \cdot 7\text{H}_2\text{O}$ was not added in the medium because multivalent cations cause the silica to gel. In Process II, a BC hydrogel was produced as described above (see “Preparation of BC”). The BC hydrogel, which had a diameter of approximately 100 mm and a thickness of 20–30 mm, was soaked in 400 ml of 0.05–1 wt% silica sol and allowed to stand for 2–3 weeks to allow the silica particles to penetrate the BC hydrogel.

Dry BC/silica nanocomposite sheets were obtained by placing the hydrogels between porous porcelain plates and pressing slowly at 120°C. The partially dried samples were pressed again at 120 °C and 2 MPa. These hot-pressed samples were removed from the press and heated in vacuo to 70–100 °C for 1–2 days. The obtained dry BC/silica nanocomposite sheets were translucent and 50–100 μm thick. The silica content in the dry nanocomposite sheets was determined by weighing the samples before and after burning them in a crucible at 900 °C in air within a furnace.

Dynamic viscoelasticity

The dynamic viscoelastic properties of dried BC and BC/silica hybrid samples were measured using a dynamic viscoelastic analyzer (DVA-200; IT Keisoku Co.) at a frequency of 10 Hz. The storage modulus (E') and the loss tangent ($\tan \delta$) were measured as a function of temperature at a heating rate of 2 °C/min.

Stress-strain measurement

The tensile properties of dried BC and BC/silica hybrid samples were measured using a universal testing machine IM-20 (INTESCO Co., Ltd.). The crosshead speed was 10 mm/min, and the gauge length was 20 mm. Rectangular specimens of 30 × 50 mm were used. For measurements of the tensile properties, 10 specimens were measured, and the results were averaged.

X-ray diffractometry

X-ray diffractometry was performed using an X'Pert PRO MPD (Panalytical). The X-ray generator was operated at a voltage of 40 kV and a current of

40 mA, and a Ni-filtered Cu K α beam with a wavelength of 0.154 nm was used.

Atomic Force Microscopy (AFM)

AFM was performed using a Seiko Instruments SPA 400 atomic force microscope in tapping mode.

Results and discussion

We prepared BC/silica nanocomposites using two methods, which we referred to as Processes I and II. Both processes used two types of silica sol, ST 20 and ST 0, which have the same diameter (10–20 nm) but different pH's (9.5–10 and 2–4, respectively). In Process I, BC hydrogel/silica nanocomposite was prepared by culturing *Ga. xylinus* in medium containing silica sol, whereas in Process II, BC hydrogel was immersed in silica sol to allow silica particles to penetrate it. We hot-pressed these BC hydro gel/silica nanocomposites to produce dry BC/silica nanocomposite sheets and then evaluated their mechanical properties. Table 1 shows the amounts of silica particles in the nanocomposite sheets as a function of the concentration of silica sol used.

Process I

A plot of the amount of silica particles in the nanocomposite sheets prepared using Process I as a

Table 1 Relationship between concentration of silica sol and loaded amount of silica in dry BC/silica nanocomposites

Concentration of silica sol wt%	Process I		Process II	
	Concentration of silica in composites wt%		Concentration of silica in composites wt%	
	ST 0	ST 20	ST 0	ST 20
0.05	0.1	1.0	2.4	2.5
0.1	0.3	1.8	1.8	2.7
0.2	0.2	1.5	2.1	2.8
0.3	1.2	3.8	3.8	3.8
0.5	1.4	4.0	4.8	2.9
1.0	8.7	11.6	10.0	3.3
2.0	40.6	52.4	–	–

function of the concentration of silica sol in the culture medium is shown in Fig. 1. The amount of silica loaded in the dry nanocomposites increased as the amount of silica sol in the culture medium was increased. Although a small amount of silica may be lost during hot-pressing of the hydrogel composites, it appears that the silica particles are incorporated well in the microfibrils of BC during culture. Up to 52.4% and 40.6% for ST 20 and ST 0, respectively, could be loaded in the nanocomposite sheets using a silica sol concentration of 2.0%. The amount of loaded silica at pH 2.4 (ST 0) was lower than that at pH 10 (ST 20), indicating that more cellulose is produced in acidic than alkaline conditions. Consistent with this finding, it thought that *Ga. Xylinus* are active and productive in acidic rather than alkaline environments (Takai 1988, 1992).

Figure 2 shows the temperature dependence of the dynamic viscoelasticity of dry BC/silica nanocomposites incorporating ST 20 produced by Process I. The storage modulus (E') of the BC sheet was as high as 20 GPa at -150 °C, and it decreased gradually with temperature to 9 GPa at 280 °C. Above 280 °C, the E' decreased rapidly with temperature due to simultaneous glass transition and thermal degradation. In the $\tan \delta$ curves, peaks appeared at approximately -80 °C, 110 °C, and 320 °C. These relaxations of cellulose have been examined in many studies using a variety of polysaccharides. The peak at approximately -80 °C is caused by end-group rotation, crystalline defects, or backbone-chain motion of short segments (Kararli et al. 1990) or by motion of $-\text{CH}_2\text{OH}$ side-chains (Montes et al. 1994;

Morooka and Norimoto 1991; Scandola and Ceccorulli 1985; Montes and Cavaille 1999; Butler and Cameron 2000). Nakamura et al. (1970) assigned this relaxation to the onset of some kind of local motion of small units such as side-chain motion ($-\text{CH}_2\text{OH}$) or the local motion of glucose residues.

A $\tan \delta$ peak at 110 °C accompanied by a stepwise change in E' for BC has been detected in starch at 127 °C (Butler and Cameron 2000) and in cellulose-acetate at 50–100 °C (Pizzoli et al. 1987; Scandola and Ceccorulli 1985). This relaxation may be caused by the elimination of absorbed water (Pizzoli et al. 1987; Scandola and Ceccorulli 1985) or glass transition of cellulose plasticized by absorbed water. In this temperature region, the secondary relaxation in the glassy state has been detected by dilatometry at 80–100 °C for cellulose, hemicellulose, and lignins (Ramiah and Goring 1965), at 105 °C for cellulose triacetate (Mandelkern and Flory 1951), and at 155 °C for cellulose acetate (Russel and Van Kerpel 1957). This relaxation was assigned to the rupture of weak hydrogen bonds (Ramiah and Goring 1965). At approximately 300 °C, there was sharp decrease in E' , and there was a $\tan \delta$ peak at 320 °C. This relaxation is associated with both glass transition and thermal degradation (Nakamura et al. 1970). Thermal degradation of BC has been observed at

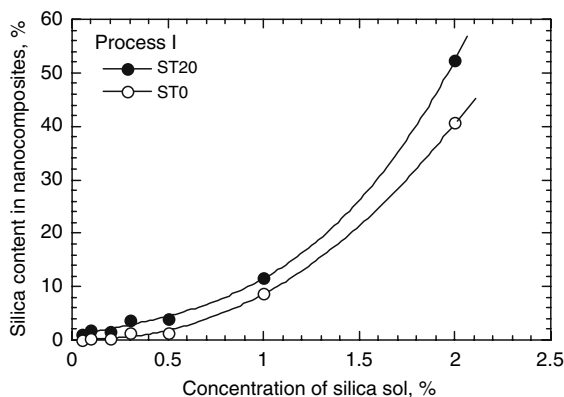


Fig. 1 Silica content in BC nanocomposites as a function of the silica sol concentration in Process I

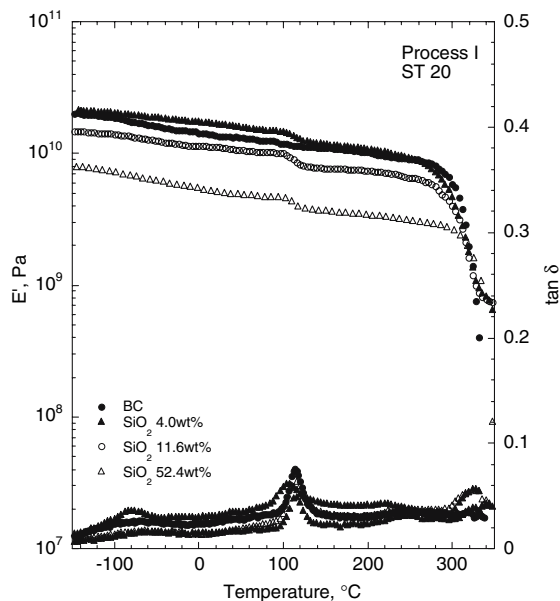


Fig. 2 Dynamic viscoelasticity of BC/silica (ST 20) nanocomposite produced by Process I

approximately 300 °C by thermogravimetry (Maeda et al. 2006).

As is seen in Fig. 2, over a wide temperature range, the E' of the BC/silica nanocomposites containing 4.0 wt% silica was larger than that of BC alone. If the silica content exceeded 11.6 wt%, however, the E' was lower. In particular, at 52.4 wt% silica, the E' decreased markedly with the temperature between -150 °C and 280 °C. The same tendency was observed when silica sol ST 0 was used.

Figure 3 shows a plot of the E' at 20 °C for the composites made of ST 20 and ST 0 as a function of the amount of silica in the nanocomposites. The E' initially increased with the silica content up to 4.0 wt% for ST 20 and 8.7 wt% for ST 0. In this region, BC may be reinforced by adding silica as a result of hydrogen bonds between OH groups on the silica surface and BC. Above 4.0 wt% ST 20 and 8.7 wt% ST 0, however, the E' of the composites decreased with the silica content and became lower than for BC alone (15 MPa). Usually, loading a matrix with fillers with a higher modulus (e.g., silica) should increase the modulus; however, above the maxima (15 wt% for ST 0 and 9 wt% for ST 20), the modulus of the composite was lower than that of matrix alone (15 GPa).

Figure 4 shows the tensile strength at 25 °C and 30% RH as a function of the silica content in the BC nanocomposites made with ST 0 or ST 20. The strength of the composite loaded with ST 20 decreased with the silica content, whereas using ST 0, the tensile strength initially increased with silica content, reaching a maximum of 192 MPa at 1.4 wt% silica. Above the maximum, the strength markedly decreased to 40 MPa at 40.6% silica content. The E' and the tensile strength of the composite produced using ST 0 were always higher than for composites produced using ST 20. This may be due to a difference in the pH of the silica sol (pH 2.4 for ST 20 and pH 10 for ST 0). As reported by Takai (1988, 1992), *Ga. Xylinus* are more active and productive in acidic than in alkaline conditions; therefore, a more dense BC hydrogel may be produced by including ST 0 in the medium.

As seen in Figs. 3 and 4, at higher concentrations of silica, E' and the strength of nanocomposites made using both ST 0 and ST 20 decreased to levels lower than for the BC matrix itself. According to the mixing

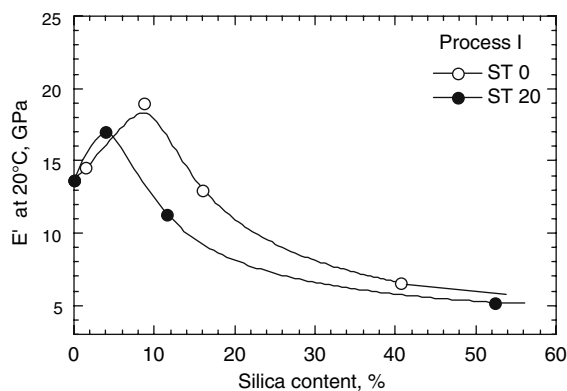


Fig. 3 E' at 20 °C as a function of silica content in BC nanocomposites made of ST 20 and ST 0 in Process I

rule, if the modulus and strength of the modulus of filler are higher than those of the matrix, the modulus and strength of the composite should be higher than for the matrix. In contrast to this rule, the E' and strength of the composites were lower than for the BC matrix at higher silica concentrations. This may be due to the disruption of the assembly of cellulose microfibrils into ribbons at high silica concentrations.

Like wood cellulose, BC membrane has a cellulose I structure, and in the X-ray diffraction pattern of dry BC, peaks appear at $2\theta = 14.5^\circ$, 16.5° , and 22.5° for $(1\bar{1}0)$, (110) , and (020) planes, respectively. In dried BC membrane, however, the $(1\bar{1}0)$ plane has a selective uniplanar orientation, and the $(1\bar{1}0)$ peak at $2\theta = 14.5^\circ$ becomes much larger. Takai et al. (1975) reported that cellulose crystals become

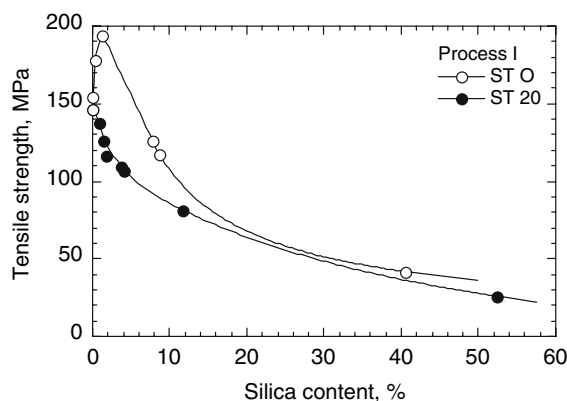


Fig. 4 Tensile strength at 25 °C and 30% RH as a function of the silica content in BC nanocomposites made of ST 20 and ST 0 in Process I

preferentially oriented in the $(1\bar{1}0)$ plane when water is removed from BC membrane. Also, replacement of the water in BC membrane with organic solvents prior to drying influences the orientation of the $(1\bar{1}0)$ plane. Polar solvents such as acetone and pyridine gave a higher selective uniplanar orientation, resulting in an increase in the intensity of the $(1\bar{1}0)$ peak, whereas nonpolar solvents such as carbon tetrachloride and cyclohexane disturb the orientation, and the intensity of the $(1\bar{1}0)$ peak decreases.

A previous study showed that BC composites can be prepared by adding water-soluble polymers such as CMC, HEC, MC, and CM-chitin to the medium (Takai 1994). The presence of water-soluble

polymers in BC membranes influences the preferential orientation of the $(1\bar{1}0)$ plane. Specifically, inclusion of CM-chitin and CMC decrease the intensity of the $(1\bar{1}0)$ peak, whereas the patterns are the same for composites containing HEC and MC as for BC alone. Tajima et al. (1995) also produced BC composites by incubating *Ga. xylinus* in medium containing CMC, MC, and PEG. Inclusion of CMC and MC caused a decrease in the intensity of the $(1\bar{1}0)$ peak and affected the formation of ribbons. In contrast, the composite containing PEG had the same X-ray diffraction pattern as BC, indicating that PEG did not change the preferential orientation of the $(1\bar{1}0)$ plane. Tokoh et al. (1998) cultured *Ga. xylinus* in Hestrin-Schramm medium containing acetyl glucuronan (AC-GM) to produce a composite of AC-GM and BC. The presence of AC-GM in the medium prevented the assembly of cellulose microfibrils, resulting in a decrease in the $(1\bar{1}0)$ peak at $2\theta = 14.5^\circ$ in the X-ray diffraction pattern.

As shown in Figs. 3 and 4, at higher concentrations of silica, the E' at 20°C and the strength of the nanocomposites made using ST 0 and ST 20 were lower than of the BC matrix. This may be due to disruption of the ribbon structure by excess silica in the BC gel. Figure 5 shows the X-ray diffraction patterns of BC and BC/silica nanocomposites prepared by adding silica particles to the medium (Process I). The height of the $(1\bar{1}0)$ peak decreased as the amount of silica was increased, and the ratio of the $(1\bar{1}0)$ peak to the (020) peak was 0.53 for BC, 0.38 for ST 0 (8.7%), and 0.35 for ST 20 (52%). As shown in Fig. 6(A), cellulose microfibrils are bundled to form ribbons that are aligned parallel to the surface of the membrane, and the $(1\bar{1}0)$ plane of the cellulose crystal is preferentially oriented parallel to the surface of the ribbon. Accordingly, BC has a sharp and large

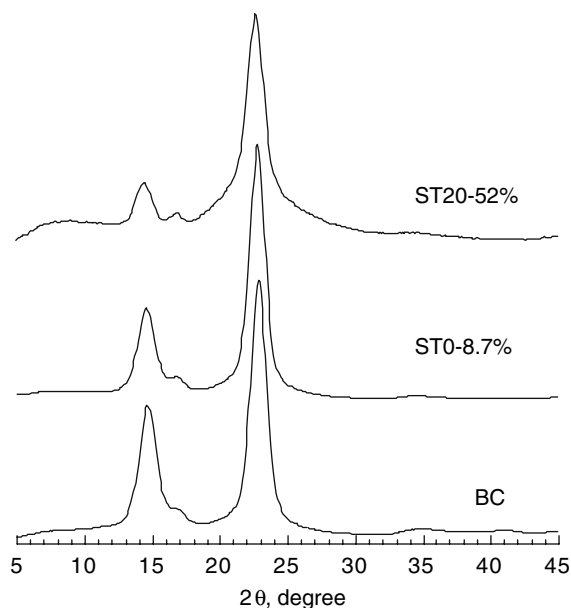
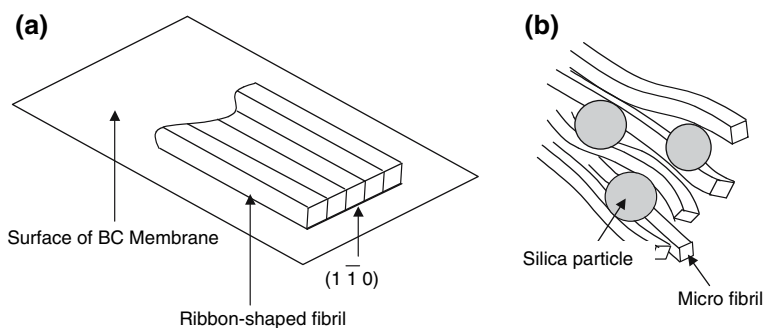


Fig. 5 X-ray diffraction patterns of BC nanocomposites produced by mixing ST 0 (8.7%) and ST 20 (52%) in Process I compared with that of BC alone

Fig. 6 Deformation of ribbon-shaped fibrils by inclusion of silica nanoparticles in Process I. (A) Complete ribbon in BC prepared without silica sol and (B) disruption of ribbon-shaped fibril formation by silica particles



(1 $\bar{1}0$) peak in the X-ray diffraction pattern. If silica particles are present in culture medium, they may disrupt the bundling of microfibrils into ribbons as shown in Fig. 6(B). Consequently the (1 $\bar{1}0$) peak of the BC nanocomposites was smaller than that for the BC matrix. In Process I, this incomplete formation of ribbons leads to a significant decrease in the modulus and strength at higher concentrations of silica.

Process II

In contrast to Process I, wherein silica is added to the culture medium, in process II, BC hydrogels are immersed in silica sol (ST 0 and ST 20) to incorporate silica particles by diffusion into the BC matrix. Figure 7 shows the silica content in dry BC/silica nanocomposites as a function of the silica sol concentration in which the BC hydrogels were immersed. Because the BC hydrogel is prepared before adding the silica sol, ribbon formation can be completed, and the silica particles are then trapped in the spaces between the ribbons. Although some of the silica sol leaks out during the process of hot-pressing, some of the silica is fixed in the BC matrix during cooling. Therefore, much less silica is incorporated in the BC using this process than Process I (Fig. 1).

Figure 8 shows an AFM image of a BC/silica nanocomposite prepared by immersing the BC hydrogel in 20% ST 0. Coagulated silica particles with a diameter of approximately 10–30 nm were present in between ribbon-shaped fibrils. The silica particles may be fixed on the ribbon through

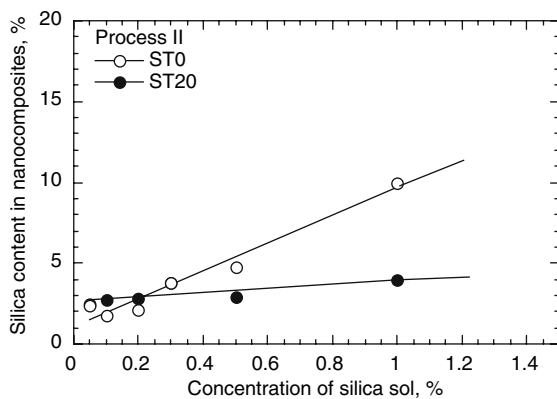


Fig. 7 Silica content in BC nanocomposites as a function of the silica sol concentration in Process II

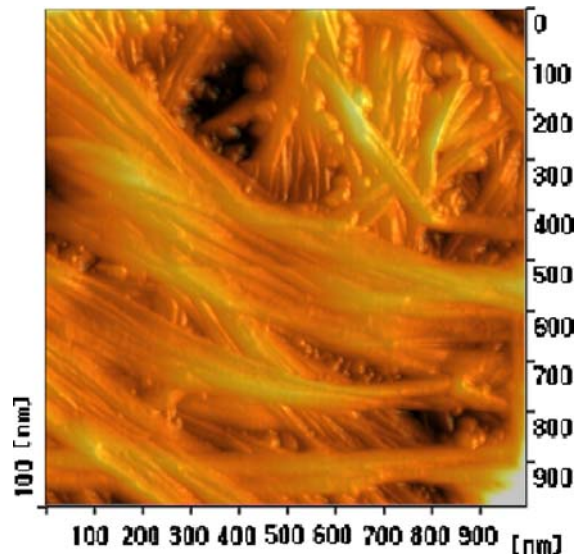


Fig. 8 AFM image of BC/silica nanocomposite prepared by Process II

hydrogen bonding between hydroxyl groups of cellulose and the surface of the silica particles.

Figure 9 shows the temperature dependence of the dynamic viscoelasticity of dry BC/silica nanocomposites produced by Process II using ST 20. The

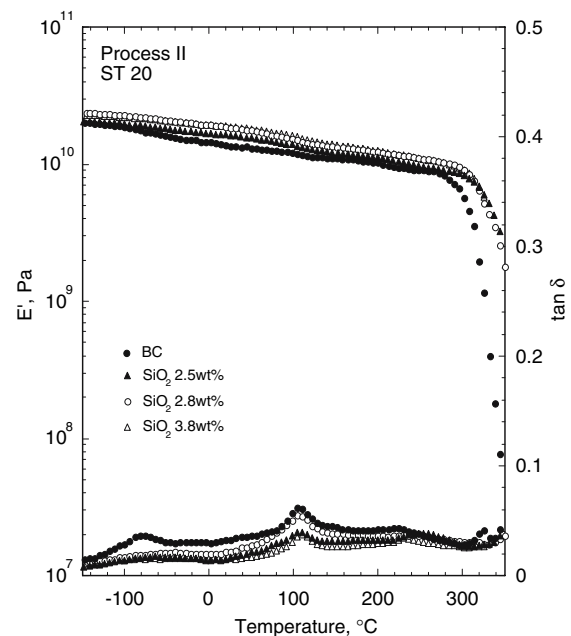


Fig. 9 Dynamic viscoelasticity of BC/silica (ST 20) nanocomposite produced by Process II

behavior of the viscoelastic properties of the composites produced by Process II is different from that produced by Process I. The E' of the composites increased with increasing silica content over the wide temperature range (-150°C and approximately 280°C). Furthermore, the E' of BC dropped near 280°C but that of the silica-containing composites shifted to approximately 300°C . This shift is due to the rise in T_g caused by restriction of the molecular motion by hydrogen bond formation between cellulose and silica particles.

In the $\tan \delta$ curves, peaks appeared at approximately -80°C , 110°C , and 320°C . The intensity of the peak at -80°C for BC, which originates from the motion of methylol groups ($-\text{CH}_2\text{OH}$), was decreased by the inclusion of silica. This suggests that hydrogen bonding occurs between the methylol group and hydroxyl groups on the surface of the silica particles. The height of the peak at approximately 100°C , which is due to the elimination of absorbed water, also decreased. This relaxation is also influenced by the formation of hydrogen bonds between cellulose and silica. The dynamic viscoelastic behavior of the composite loaded with ST 0 shows the same tendency as that loaded with ST 20.

Figure 10 shows the E' at 20°C as a function of the silica content in the BC/silica nanocomposites. The E' of the nanocomposites soaked in ST 0 and ST 20 increased markedly with the silica content up to maxima of 22 GPa for ST 0 and 19 GPa for ST 20. This increase in E' is caused by reinforcement by the silica fixed in the spaces between the ribbons by hydrogen bonding.

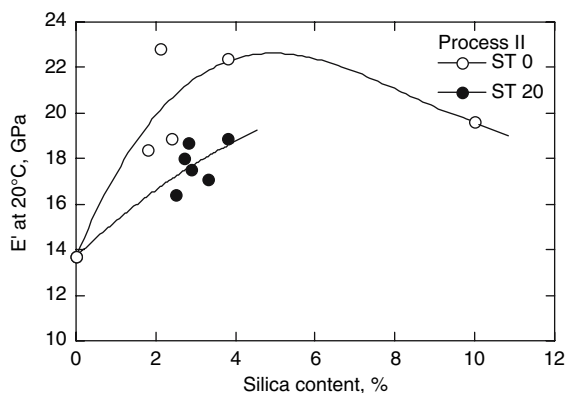


Fig. 10 E' at 20°C as a function of silica content in BC nanocomposites made of ST 20 and ST 0 in Process II

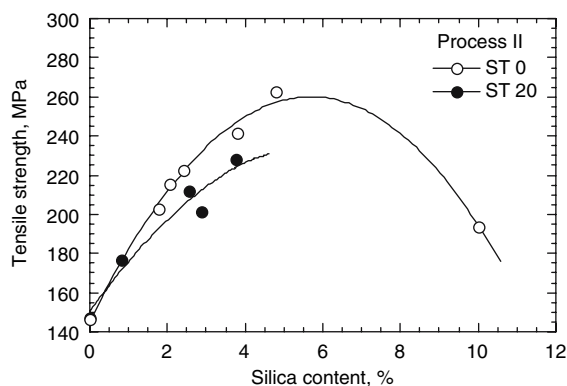


Fig. 11 Tensile strength at 25°C and 30% RH as a function of silica content in BC nanocomposites made of ST 20 and ST 0 in Process II

Figure 11 shows the tensile strength at breakage as a function of the silica content in the nanocomposites. When ST 0 was used, the tensile strength increased with the amount of incorporated silica up to a maximum of approximately 260 MPa at 4.5% silica content and then decreased to 195 MPa at 10% silica content. In the case of ST 20, the tensile strength reached 220 MPa at 4% of silica content. Amounts of silica below approximately 5% are effective at

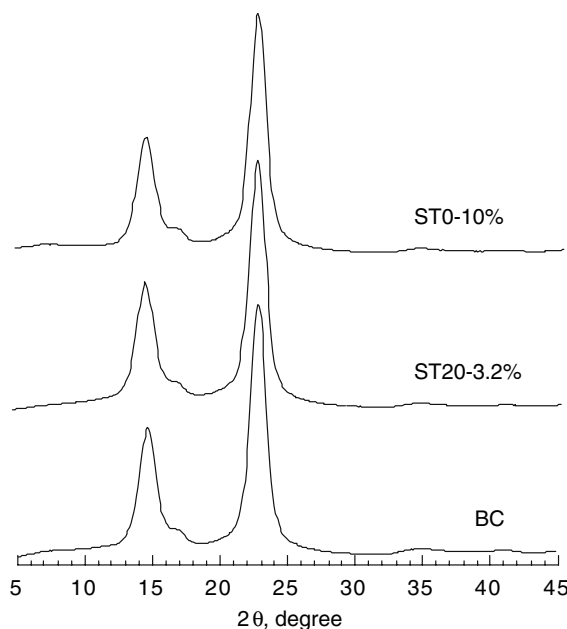


Fig. 12 X-ray diffraction patterns of BC nanocomposites produced by mixing ST 0 (10%) and ST 20 (3.2%) in Process II compared with that of BC

reinforcing the nanocomposites, but too much silica makes the composites fragile and leads to a decrease in their tensile strength. Because silica sol is not added to the medium in Process II, the formation of ribbon-shaped fibrils could proceed normally and the mechanical properties of the BC/silica nanocomposites were improved by the later incorporation of silica.

Figure 12 shows the X-ray diffractometry of BC/silica nanocomposites and BC. The height of the (1 $\bar{1}$ 0) peak was not changed by the incorporation of silica. The ratio of the (1 $\bar{1}$ 0) intensity to the (020) intensity was 0.50, 0.52, and 0.53 for BC/ST0 (10 wt%), BC/ST20 (3.2 wt%), and BC, respectively; thus, it was unaffected by the incorporation of silica.

Conclusions

BC/silica nanocomposites were prepared by two procedures using silica sols ST 0 (diameter 10–20 nm; pH 9.5–10.0) and ST 20 (diameter 10–20 nm; pH 2–4). In Process I, we added silica sol to the growth medium for *Ga. xylinus*. This resulted in the incorporation of silica particles between the microfibrils. The elastic modulus at 20 °C was improved when the nanocomposites contained less than 4% silica for ST 20 and less than 8.7% silica for ST 0. If higher amounts of silica were incorporated, however, the modulus at 20 °C and the strength of the nanocomposites were lower than for BC alone. This loss of elasticity and strength is probably due to disruption of the formation of ribbon-shaped fibrils by silica particles and a change in the preferential orientation of the (1 $\bar{1}$ 0) plane as indicated by a decrease in the peak intensity at $2\theta = 14.5^\circ$ in the X-ray diffraction pattern.

In Process II, the BC hydrogel was immersed in various concentrations of silica sol, allowing silica particles to be trapped and fixed in the spaces between completed ribbon-shaped fibrils. In this case, the modulus at 20 °C and strength were improved compared to BC alone; however, it was difficult to load the BC composite with more than 10% silica.

In both processes, the modulus at 20 °C and the strength of the BC nanocomposites made using ST 0 (pH 2–4) were always higher than for those of the nanocomposites made using ST 20 (pH 9.4–10). This is because *Ga. xylinus* are more active and productive in an acidic than an alkaline environment.

References

- Astley OM, Chanliaud E, Donald AM, Gidley MJ (2003) Tensile deformation of bacterial cellulose composites. *Int J Biol Macromol* 32:28–35
- Atalla RH, Hackney JM, Uhlin I, Thompson NS (1993) Hemicelluloses as structure regulators in the aggregation of native cellulose. *Int J Biol Macromol* 15:109–112
- Azuma J (1999) Composite formation of cellulose with hemicellulose. *Cellulose Commun* 6:12–17
- Butler MF, Cameron RE (2000) A study of the molecular relaxations in solid starch using dielectric spectroscopy. *Polymer* 41:2249–2263
- Fontana CK, Torriani IL, Moreschi JC, Galloti BJ, de Souza SJ, Narcisco GP, Bichara JA, Farah LF (1990) *Acetobacter* cellulose pellicle as a temporary skin substrate. *Appl Biochem Biotechnol* 24–25:253–264
- Haigler CH, Brown RM Jr, Benziman M (1980) Calcofluor white ST alters the in vivo assembly of cellulose microfibrils. *Science* 210(4472):903–906
- Hayashi T, Marsden MPF, Delmar DP (1987) Pea xyloglucan and cellulose. V. Xyloglucan-cellulose interactions in vitro and in vivo. *Plant Physiology* 83:384–389
- Hioki N, Hori Y, Watanabe K, Morinaga Y, Yoshinaga F, Hibino Y, Ogura T (1995) Bacterial cellulose as a new material for papermaking. *Japan TAPPI J* 49:718–723
- Ichikawa H (1995) Recent development of the speaker cone paper. *Sen-i Gakkaishi* 51:397–401
- Iguchi M, Yamanaka S, Budhiono A (2000) Bacterial cellulose— a masterpiece of nature's arts. *J Mater Sci* 35:261–270
- Iwata T, Lucia I, Azuma J (1998) Affinity of hemicellulose for cellulose produced by *Acetobacter xylinum*. *Cellulose (London)* 5(3):215–228
- Kai A (1989) Present prospect and problems of study on bacterial cellulose. *Japan TAPPI J* 43:441–454
- Kai A, Kobayashi T (1992) Influence of poly(vinyl alcohol) on the structure of bacterial cellulose spherulite. *Polymer J* 24:131–133
- Kararli TT, Hurlbut JB, Needham TE (1990) Glass-rubber transitions of cellulosic polymers by dynamic mechanical analysis. *J Pharmaceutical Sci* 79(No. 9):845–848
- Maeda H, Nakajima M, Hagiwara T, Sawaguchi T, Yano S (2006) Bacterial cellulose/silica hybrid fabricated by mimicking biocomposites. *J Mater Sci* 41:5646–5656
- Mandelkern L, Flory PJ (1951) Melting and glassy state transitions in cellulose esters and their mixtures with diluents. *J Am Chem Soc* 73:3206–3212
- Montes H, Cavaille JY (1999) Secondary dielectric relaxations in dried amorphous cellulose and dextran. *Polymer* 40:2649–2657
- Montes H, Cavaille JY, Mazeau K (1994) Secondary relaxations in amorphous cellulose. *J Non-Crystalline Solids* 172–174:990–995
- Morooka T, Norimoto M (1991) Viscoelastic properties of dialcohol cellulose prepared by homogeneous periodate oxidation. *Sen-i Gakkaishi* 47(7):328–333
- Nakamura S, Gillham JK, Tovolsky AV (1970) Torsional Braid analysis of cellulose. *Rep Prog Polym Phys Jpn* XIII:89–90

- Pizzoli M, Scandora M, Ceccorulli G (1987) Viscoelastic relaxations of cellulose acetate in the solid state. In: Kennedy JF, Phillips GO, Williams PA (eds) Wood and cellulose: industrial utilization, biotechnology, structure and properties. John Wiley & Sons, New York, Chichester, Brisbane, Toronto, Chapter 11
- Ramiah MV, Goring DAI (1965) The thermal expansion of cellulose, hemicellulose, and lignin. *J Polym Sci: Part C* 11:27–48
- Romano M, Seves A, Tsukada M (1992) Physical properties of native cellulose from *Acetobacter xylinum*. *Cellulose Chem Technol* 26:379–386
- Russel J, Van Kerpel RG (1957) Transitions in plasticized cellulose acetates. *J Polym Sci* 25:77–96
- Scandola M, Ceccorulli G, (1985) Viscoelastic properties of cellulose derivatives: 1. Cellulose acetate. *Polymer* 26:1953–1957
- Seifert M, Hesse S, Kabrelian V, Klemm D (2004) Controlling the water content of never dried and reswollen bacterial cellulose by the addition of water soluble polymers to the culture medium. *J Polym Sci: Part A: Polym Chem* 42:463–470
- Shibazaki H, Kuga S, Onabe F (1994) Mechanical properties of papersheet containing bacterial cellulose. *Japan TAPPI J* 48:1621–1630
- Tajima K (1999) Development of biodegradable materials from bacterial cellulose. *Biosci Ind* 57:391–394
- Tajima K, Fujiwara M, Takai M, Hayashi J (1995) Synthesis of bacterial cellulose composite by *Acetobacter xylinum* I. Its mechanical strength and biodegradability. *Mokuzai Gakkaishi* 41:749–757
- Takai M (1988) Bacterial cellulose. *Japan TAPPI J* 42:237–244
- Takai M (1992) Biosynthesis and Applications of Bacterial Cellulose. *Sen-i Gakkaishi* 48:153–157
- Takai M (1994) Bacterial cellulose composites. In: Gilbert RD (ed) Cellulose polymer blends composites. Hanser, Munich, pp 233–240, Chapter 13
- Takai M, Tsuta Y, Hayashi J, Watanabe S (1975) Biosynthesis of cellulose by *Acetobacter xylinum* III. X-ray studies of preferential orientation of the crystallites in a bacterial cellulose membrane. *Polymer J* 7(2):157–164
- Tokoh C, Takabe K, Fujita M, Saiki H (1998) Cellulose synthesized by *Acetobacter xylinum* in the presence of acetyl glucomannan. *Cellulose* 5:249–261
- Tokoh C, Takabe K, Sugiyama J, Fujita M (2002) CP/MAS ¹³C NMR and electron diffraction study of bacterial cellulose structure affected by cell wall polysaccharides. *Cellulose* 9:351–360
- Yamanaka S, Watanabe K, Kitamura N, Iguchi M, Mitsuhashi S, Nishi Y, Uryu M (1989) The structure and mechanical properties of sheets prepared from bacterial cellulose. *J Mater Sci* 24:3141–3145
- Yamanaka S, Watanabe K, Iguchi M, Nishi Y (1998) Production, properties, and application of bacterial cellulose. *Nippon Nokeikagaku Kaishi* 72:1039–1044
- Yoshino K, Matsuoka R, Nogami A K, Araki H, Yamanaka S, Watanabe K, Takahashi M, Honma M (1991) Electrical property of pyrolyzed bacterial cellulose and its interaction effect. *Synthetic Mater* 42(1–2):1593–1599
- Watanabe K, Yamanaka S (1992) Cellulose produced by bacteria. *Biosci Ind* 50:534–541